J. Mt. Sci. (2014) 11(6): 1385-1395 e-mail: jms@imde.ac.cn http://jms.imde.ac.cn
DOI: 10.1007/s11629-014-3051-z

Mutual Interference of Two Debris Flow Deposits Delivered in a Downstream River Reach

STANCANELLI Laura Maria[1]*, LANZONI Stefano[2], FOTI Enrico[1]

1 Department of Civil Engineering and Architecture, University of Catania, Catania I95123, Italy

2 Department of Civil, Environmental and Architectural Engineering, University of Padua, Padua I35131, Italy

**Corresponding author, e-mail: lmstanca@dica.unict.it*

Citation: Stancanelli LM, Lanzoni S, Foti E (2014) Mutual interference of two debris flow deposits delivered in a downstream river reach. Journal of Mountain Science 11(6). DOI: 10.1007/s11629-014-3051-z

Abstract: We investigate experimentally the depositions of two contiguous debris flows flowing into a main river reach. The aim of the present experimental research is to analyze the geometry and the mutual interactions of debris flow deposits conveyed by these tributaries in the main channel. A set of 19 experiments has been conducted considering three values of the confluence angle, two slopes of the tributary, and three different triggering conditions (debris flows occurring simultaneously in the tributaries, or occurring first either in the upstream or in the downstream tributary). The flow rate along the main channel was always kept constant. During each experiment the two tributaries had the same slope and confluence angle. The analysis of the data collected during the experimental tests indicates that the volume of the debris fan is mainly controlled by the slope angle, as expected, while the shape of the debris deposit is strongly influenced by the confluence angle. Moreover, in the case of multiple debris flows, the deposit shape is sensitive to the triggering conditions. Critical index for damming formation available in literature has been considered and applied to the present case, and, on the basis of the collected data, considerations about possible extension of such indexes to the case of multiple confluences are finally proposed.

Keywords: Debris flows; Confluences; Dam formation; Triggering scenario; Critical Index

Received: 6 May 2014
Accepted: 10 October 2014

Introduction

Debris flows formed in the headwaters of mountain basins usually move downstream, entraining further sediments along their paths, and finally deposit on lower slopes often obstructing or even damming the section of lower gullies. The accumulation of such deposits represents a rich source of material for subsequent dangerous debris flows formation, as it is often observed in nature. A relevant example of this kind of phenomena is the Wenjiagou gully event in China (Zhou et al. 2013).

Due to the great impact on the hydraulic and hydrological features of the receiving river, with the possible formation of a dam and its subsequent catastrophic failure, the confluence of a debris flow into a downstream river has been studied by many authors. In particular, the analysis of a confluence between a tributary debris flow and a main stream, leading to the formation of a deposit in the receiving channel, has been analyzed following empirical, probabilistic and numerical approaches. Benda et al. (1990) synthesized some field observations related to the geometry of stream junctions into a simple relation for predicting travel distance and volume of debris flows in confined mountain channels. Li et al. (2008) proposed a probabilistic approach to assess the risk of a gully area. More specifically, the occurrence of an obstruction in the mainstream is associated with the probability of confluence of tributary flows, carrying out a certain amount of debris flow discharge, and with the size of valley hosting the mainstream. Numerical models have also been used to determine the spatial distribution of velocities and water depths in the main river as a consequence of the sediment deposits generated by the debris flows delivered by tributaries (Chen et al. 2011). Other studies, focused on the analysis of the blockage of the main river, suggest critical indexes for dam formation on the basis of both empirical and experimental approaches (Swanson 1985, 1986; Ermini et al. 2006; Dal Sasso et al. 2014; Dang et al. 2009).

Empirical approaches (see, e.g., Swanson 1985, 1986; Ermini et al. 2006; Dal Sasso et al. 2014) rely on field data, and provide critical indexes for dam formation based on key factors such as: the discharge ratio between the tributary and the main stream, the bulk density of the debris flow, the channel slope, the confluence angle and the degree of sediment sorting. The experimental approach (Dang et al. 2009) try to schematize the relevant natural processes under controlled conditions, in order to find specific critical indexes that can be used to assess the probability of dam formations for a given tributary. In particular, the laboratory experiments performed by Dang et al. (2009) for a single confluence indicate that the probability that a debris dam forms in the receiving channel are strictly related to the discharge and velocity ratios between the tributary and the main stream, the bulk density of the debris flow, the confluence angle and degree of unevenness of grain size. Depending on the value attained by the some relevant dimensionless indexes, three types of blockage in the main channel have been documented by Dang et al. (2009): i) semi blockage; ii) semi blockage where the deposit was partially immersed under the stream flow; iii) complete blockage.

The present contribution aims at obtaining experimental information on the interaction of multiple debris flows which flow into the same recipient river reach at relatively small distances, determining the formation of significant sediment deposits. The degree of obstruction of the receiving channel is evaluated by considering the effects of tributary slope, confluence angle and different triggering scenarios. Such a study has been inspired by a real case, occurred in the Messina Province (Italy) on October 1st, 2009. The mutual interactions between three different nearly simultaneous debris flows produced dramatic effects in terms of loss of human lives and damages in the Giampilieri town, located on the left side of the Giampilieri stream. The three tributaries involved in the catastrophic event were the Loco, the Sopra Urno and the Puntale creeks, crossing the urbanized area of Giampilieri and all debouching into the Giampilieri stream. All tributary creeks are characterized by small catchment basins (1 km^2, 0.7 km^2 and 0.4 km^2, respectively) and join the Giampilieri stream at distances of few hundreds of meters. Their contribution to the discharge flowing in the Giampilieri is usually quite low or even negligible. Nevertheless, during the particularly intense precipitations that characterized the alluvial event of October 1st, 2009, nearly simultaneous debris flows were conveyed in the three tributaries, inundating the urbanized area they crossed and eventually flowing into the Giampilieri river. The need to design suitable mitigation structures and a confluence geometry that hopefully minimizes the effects of future debris flow events inspired the present investigation. In order to individuate the most dangerous configuration, we considered the geometry of the sediment deposits in the main receiving channel, evaluating the location of the center of mass, the volume and the shape of the sediment deposits. For the sake of simplicity, the experiments have been carried out by using a gravel material. This choice allows one to simplify significantly the degree of complexity of the process, focusing on conditions typical of stony debris flows. This type of debris flows is very common in mountain headwaters (Rickenmann and Recking 2011), in particular on the Dolomites (northern Italy), where multiple debris flows have been often documented (Gregoretti and Dalla Fontana 2008).

The paper is organized as follows. In the next section the experimental set-up and procedure are presented. The experimental setup and procedures are described in Section 2. The results of the experiments are presented in section 3, with particular attention to the analysis of the data concerning the volume and shape of the deposits forming in the main channel, determining a certain degree of obstruction. Finally, Section 4 reports the conclusions.

1 Experimental Set Up and Procedure

The investigations have been performed at the Hydraulic Laboratory of the Department of Civil, Environmental and Architectural Engineering of the University of Padua (Italy). The experimental apparatus has been designed in order to study the triggering, propagation and deposition of debris flows generated along two different tributary channels, close to each other, which conveyed their debris-water mixtures into a river reach located downstream (Figure 1).

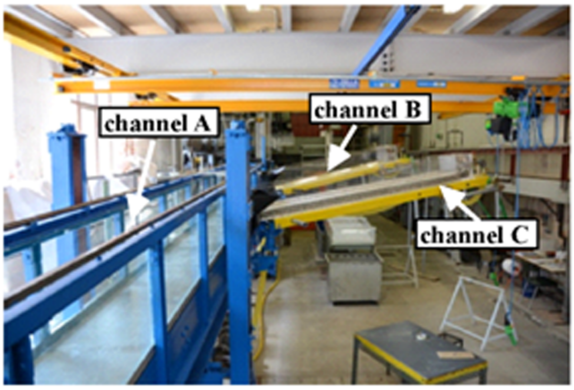

Figure 1 Overview of the experimental apparatus composed by a main channel (A) and two tributary channels (B and C).

The experimental set up includes a main channel reach (denoted hereinafter as channel A) 12 m long, 0.5 m wide and with a depth of 0.70 m; and two lateral channels, called respectively channel B (upstream) and channel C (downstream), that have a length of 3 m, a width of 0.3 m, and a depth of 0.30 m. The tributary channels B and C are located on the left side of the main channel, at an inter-axis distance of about 2.7 m, and are connected to it by means of a joint system which allows the tributary slopes and the confluence angles to vary at a large extent.

The bottom surface of all the channels was roughed by gluing a layer of the granular material used in the experiments. Before every experiment, the two tributaries were filled with a layer of sediments of thickness in a range 9-10 cm. A Plexiglas box, filled with coarse gravel, placed at the upstream section of each tributary, and a small permeable sill, located at the downstream tributary end, ensured the gradual saturation of the initial sediment layer before every experiment, preventing bed degradation.

The sediment used to generate the debris flow was composed by nearly uniform fine gravel, with grain diameter varying in a range 2-5 mm. Table 1 describes the main characteristics of such material, namely: the range of gravel diameters *d*, the immersed specific weight γ_S, the porosity n, the mean dry and submerged angle of repose, φ_D and φ_S, the standard deviation σ of the latter, and the hydraulic conductivity *K*.

Table 1 Physical, mechanical, and hydraulic characteristics of the fine gravel adopted in the experiments.

d [mm]	γ_S [N/m³]	n [-]	φ_D [°]	φ_S [°]	σ [°]	*K* [m/s]
2-5	17.440	0.38	48.6	43.3	0.5	0.001

Notes: d: gravel diameter range; γ_S: immersed specific weight; n: porosity; φ_D: mean dry angle of repose; φ_S: submerged angle of repose; σ: standard deviation of angle of repose; K: hydraulic conductivity.

Six acoustic level sensors (ensuring an error smaller than 0.001 m) have been installed along the various channels in order to monitor flow levels during the propagation and deposition of the debris flows. In particular, the sensors have been located along channel A, B and C, in proximity of the confluences.

The dimensions of the experimental apparatus were chosen on the basis of a preliminary study of the debris flow regime that can be reproduced in the tests. As previously stated we concentrated our attention on stony debris flows (Takahashi 2007). Moreover, we wanted to reproduce mature debris flow conditions, whereby the grains were dispersed throughout the entire flow depth. This type of flow was obtained by choosing relatively high slope angles of the tributaries and a large enough triggering water discharge (Lanzoni and Tubino 1993). The criterion proposed by Takahashi (2007), as well as visual observations, were used to classify the observed debris flow regime.

The experimental procedure (Figure 2) consists of a preliminary phase needed to fix the geometrical configuration of the experimental apparatus, namely the slopes and the confluence angles of the tributaries (set equal for both

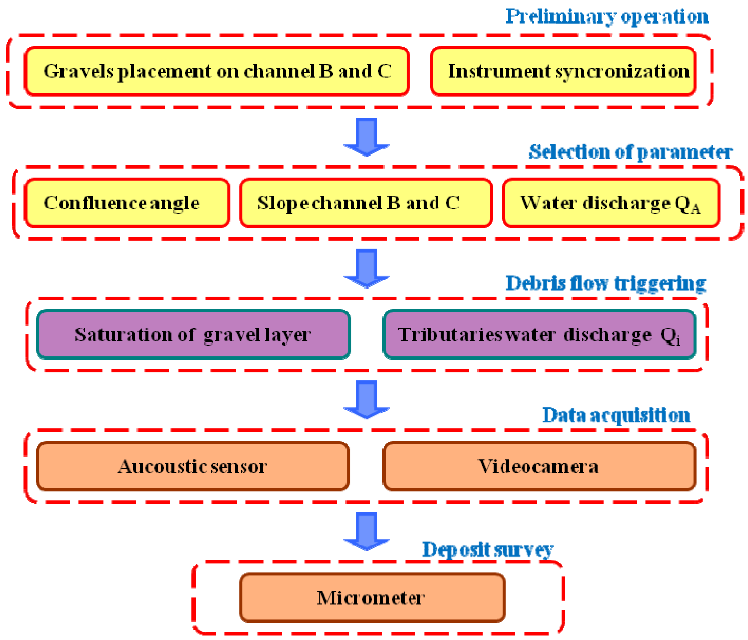

Figure 2 Diagram box indicating the applied experimental procedure.

channels), as well as the slope (5°) and the water discharge (5 L/s) of the main channel. Afterward, a sediment layer of thickness in a range 9-10 cm was placed into the tributaries and compacted manually. In order to facilitate the experiment preparation the material needed for a given experiment was moved by means of an overhead traveling crane and a hopper. The sediment layer was saturated with a very low discharge about 0.8 L/s. In each tributary, the debris flow was triggered by releasing a prescribed water discharge Q_i into a Plexiglas box located at the channel head. The debris flow then propagated over the erodible bed, which was eventually washed out, and deposited within the main receiving channel.

The sediment mobilized by the debris flow was eventually deposited into the main channel and progressively shaped by the water flowing along it.

During each experiment it was possible to recognize three different zones within the deposits: an upstream area shaped by the main channel flow; an intermediate zone where the depositional fan was essentially determined by debris flow inertia, and a downstream area where the eroded sediment was progressively washed out. These deposit characteristics resemble those observed by Cheng et al. (2007) in the case of a single debris flow joining a main river with lower slope. The experiment ended when the geometry of the deposits did not change appreciably.

2 Experiments

The experiments consisted of 19 runs, although some preliminary analyses have been carried out in order to select the tributary slopes ensuring mature debris flow conditions. The mixture of water (density 1000 kg/m3) and sediment (density 2650 kg/m3) propagating along the tributary channels was characterized by a bulk concentration varying in the range 0.3-0.4, depending on the tributary slope angle. The mean debris flow velocity varied from 0.5 to 1 m/s. Table 2 reports the relevant hydraulic and geometric parameters characterizing the tests: the reference number, the tributary slope angle β, the water discharge Q_i, the confluence angle α and the time t_0 at which debris flow were triggered in the tributary channels. In particular, we tested three different confluence angles (90° - 60° - 50°), two different tributary slopes (15° and 17°), and three different triggering conditions: debris flows generated first on the upstream tributary and then downstream tributary (scenario I); debris flows generated first on the downstream tributary and then on the upstream tributary (scenario II); occurring simultaneously in the tributaries (scenario III). The water discharge Q_A along the main channel was kept almost constant in the various tests, even though it plays an important role in shaping the sediment deposits. Indeed, an increase of water discharge along the main channel (experiments 6 and 7) caused an increased erosion of the sediment deposited on the main channel.

The duration of each experiment was found to depend on the thickness of the layer initially placed in the tributary flumes and on the tributary slopes (Lanzoni and Tubino 1993). The sediment concentration of the sediment-water mixture was not fixed in advance, but resulted from the entrainment of sediment from the erodible sediment layer initially placed in the channels. Finally, at the end of each test the geometry of the deposition fans formed in the main channel was carefully surveyed along 5 different longitudinal transects, 5 m long and 10 cm apart from each other, in order to cover the entire area of the main channel influenced by the confluence deposits.

Figure 3 shows the debris flow fan observed at the end of test 2. In particular, Figure 3a presents a view of the main channel, looking from downstream, while Figure 3b reports the three-dimensional recon-struction of the sediment deposit. Figure 3a clearly shows the formation of two main deposits along the main channel where the two confluences are located, and a secondary one (about 20 cm wide) in between them, indicated with a blue arrow, resulting from the interaction between the two debris flow deposits, which are shaped by the water flowing in the main channel. A secondary deposit is formed along the main channel wall opposite to the confluences. The longitudinal extension of this secondary deposit (Figure 3b) is about 50 cm (1.5 times the channel width) while its width is of the order of 5 cm.

Table 2 **Geometric and hydraulic parameters adopted during the experimental campaign**

N. test	channel A		channel B				channel C			
	β_A	Q_A [L/s]	β_B	α_B	t_B [s]	Q_B [L/s]	β_C	α_C	t_C [s]	Q_C [L/s]
1	5°	5.0	17°	60°	0	3.4	17°	60°	168	3.2
2	5°	5.2	17°	60°	176	3.4	17°	60°	0	3.2
3	5°	5.1	17°	60°	0	3.4	17°	60°	0	3.2
4	5°	5.2	17°	50°	0	3.4	17°	50°	175	3.2
5	5°	5.1	17°	50°	222	3.4	17°	50°	0	3.2
6	5°	5.1	17°	50°	0	3.4	17°	50°	0	3.2
7	5°	6.0	17°	50°	0	3.4	17°	50°	0	3.2
8	5°	5.0	15°	50°	0	3.4	15°	50°	210	3.2
9	5°	5.0	15°	50°	227	3.4	15°	50°	0	3.2
10	5°	5.1	15°	60°	0	2.8	15°	60°	0	2.8
11	5°	5.1	15°	60°	0	2.8	15°	60°	214	2.7
12	5°	5.1	15°	60°	219	2.8	15°	60°	0	2.7
13	5°	5.0	15°	50°	0	2.7	15°	50°	0	3.0
14	5°	5.1	15°	90°	0	2.8	15°	90°	0	2.9
15	5°	5.1	17°	90°	0	3.1	17°	90°	0	2.8
16	5°	5.1	17°	90°	0	3.1	17°	90°	235	2.9
17	5°	5.1	17°	90°	158	3.1	17°	90°	0	2.9
18	5°	5.0	15°	90°	0	3.1	15°	90°	206	3.0
19	5°	4.8	15°	90°	204	3.0	15°	90°	0	2.9

Notes: β_A: slope angle of main channel A; Q_A: water discharge along the main channel A; β_B: slope angle of tributary channel B; α_B: confluence angle of tributary B; t_B: triggering time in the tributary channel B; Q_B: water discharge along the tributary channel B; β_C: slope angle of tributary channel C; α_C: confluence angle of tributary C; t_C: triggering time in the tributary channel C; Q_C: water discharge along the tributary channel C.

3 Analysis of Results

The deposit surveyed along the main channel have been firstly analyzed by considering some characteristic parameters, such as the volume and center of mass of each debris fan (corresponding to the upstream and downstream

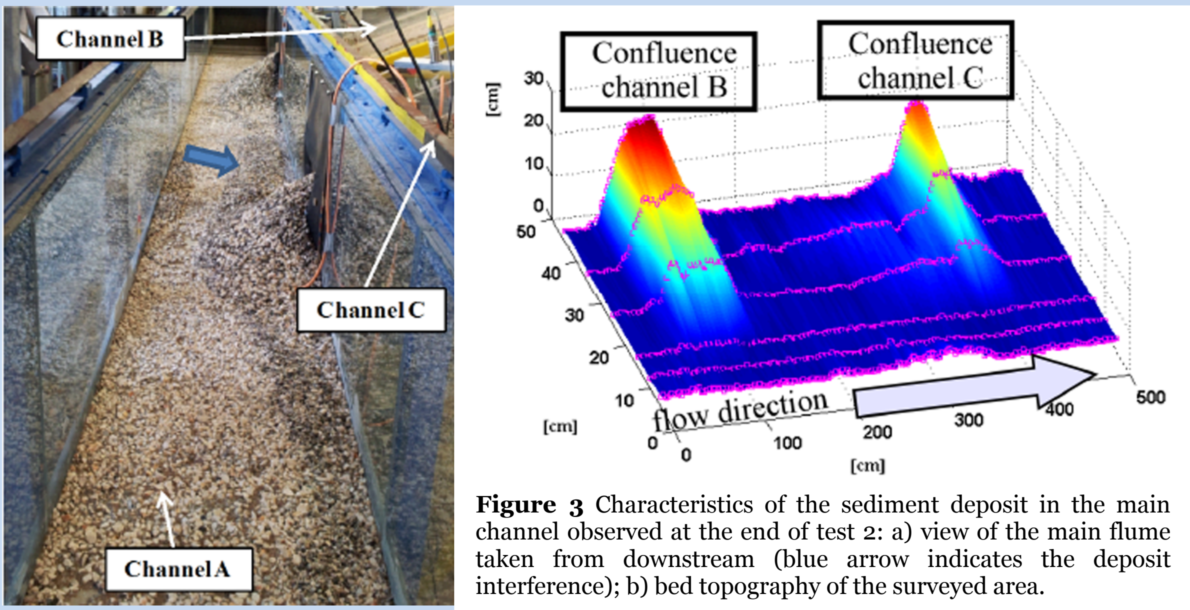

Figure 3 Characteristics of the sediment deposit in the main channel observed at the end of test 2: a) view of the main flume taken from downstream (blue arrow indicates the deposit interference); b) bed topography of the surveyed area.

confluences) and of the entire deposit. The contour lines of the overall material deposited along the main channel were also studied. The aim was to quantify objectively the influence of the various parameters (confluence angle, slope angle and triggering scenario) on the degree of obstruction of the main channel. With respect to this, various critical indexes for damming prediction have also been considered.

3.1 Analysis of the characteristic parameters of the sediment deposit along the main channel

In order to allow a systematic and objective comparison among the sediment deposits formed in the different tests, the following parameters have been considered:

- overall volume of the sediment deposited within the main channel, V_{dep};
- location of the center of mass of this volume, (X_G, Y_G, Z_G);
- location of the center of mass of the debris fans formed in proximity of each confluence: upstream (X_{GB},Y_{GB},Z_{GB}), downstream (X_{GC}, Y_{GC}, Z_{GC}).

Table 3 summarizes the values attained by these parameters in each test. Figure 4 shows the slope angle versus the volume of material deposited along the main channel for all the tests. As already observed by Chen et al. (2004), the debris volume is slightly related to the confluence angle, but is significantly influenced by the tributary slope. On the other hand, its shape is markedly affected by the confluence angle, in accordance with observations carried out by Chen et al. (2004) in the case of a single confluence. Figure 5 shows a plan view of the position of the center of mass (for each fans and for the overall deposit) for the same tributary slope angle (17°) and different confluence angle. In particular, Figures 5a, 5b and 5c refer to the triggering scenarios I, II and III, respectively. In general, for the confluence corresponding to the upstream fan, the higher the confluence angle (e.g., 90°), the more the center of mass shifts towards to the opposite confluence wall, thus indicating a larger degree of damming. This behavior conforms to that observed in the case of a single confluence. Nevertheless, in case of multiple, relatively close confluences, as considered here, the location of the center of mass of the downstream deposit varies significantly in relation to the triggering scenario. Conversely, the location of the center of mass of the upstream deposit is only slightly affected by different triggering conditions. In other words, the triggering scenario is found to strongly influence

Table 3 Characteristic parameters of the sediment deposits observed in each test

TEST n°	V_{dep} [cm³]	X_G [cm]	Y_G [cm]	Z_G [cm]	X_{GB} [cm]	Y_{GB} [cm]	Z_{GB} [cm]	X_{GC} [cm]	Y_{GC} [cm]	Z_{GC} [cm]
1	100,787.2	262.6	29.8	10.9	82.0	30.7	10.6	390.4	29.1	11.2
2	103,424.6	241.2	30.6	8.6	88.4	30.9	11.5	348.3	30.5	6.5
3	97,562.6	238.4	32.0	7.3	105.3	30.6	7.5	353.3	33.3	7.1
4	101,705.2	257.1	31.3	9.2	101.6	30.7	9.7	402.7	31.9	8.8
5	98,036.8	262.7	31.1	8.9	98.2	31.5	10.0	397.0	30.8	8.0
6	96,802.6	238.3	30.6	8.3	111.2	30.0	9.2	386.4	31.3	7.2
7	101,374.4	257.6	31.9	6.3	-	-	-	-	-	-
8	90,283.4	240.3	32.1	7.7	118.0	31.6	7.7	378.2	32.8	7.7
9	85,255.2	261.2	32.2	6.7	111.0	31.0	9.0	383.2	33.1	4.9
10	105,948.6	258.1	31.4	7.8	-	-	-	-	-	-
11	90,983.6	259.2	32.0	7.7	-	-	-	-	-	-
12	94,488.6	244.2	31.9	7.9	-	-	-	-	-	-
13	86,464.6	258.0	32.3	7.0	-	-	-	-	-	-
14	85,878.8	251.3	32.4	7.7	-	-	-	-	-	-
15	106,990.8	270.5	28.5	7.0	117.3	30.1	8.2	349.6	27.7	6.3
16	101,054.2	245.6	31.0	8.8	108.7	30.3	8.5	367.8	31.7	9.2
17	99,373.8	260.2	29.6	6.9	117.1	30.3	8.1	350.5	29.2	6.1
18	105,433.2	250.7	31.3	9.7	97.8	31.1	9.7	382.0	31.4	9.8
19	105,613.46	260.2	29.6	7.4	115.3	29.8	8.4	358.9	29.5	6.8

Notes: V_{dep}, sediment deposit volume surveyed along the main channel; X_G, Y_G, Z_G, location of the center of mass for the entire deposit; X_{GB}, Y_{GB}, Z_{GB}, location of the center of mass of the single deposit formed in proximity of the upstream tributary (channel B); X_{GC}, Y_{GC}, Z_{GC}, location of the center of mass of the single deposit formed in proximity of the downstream tributary (channel C).

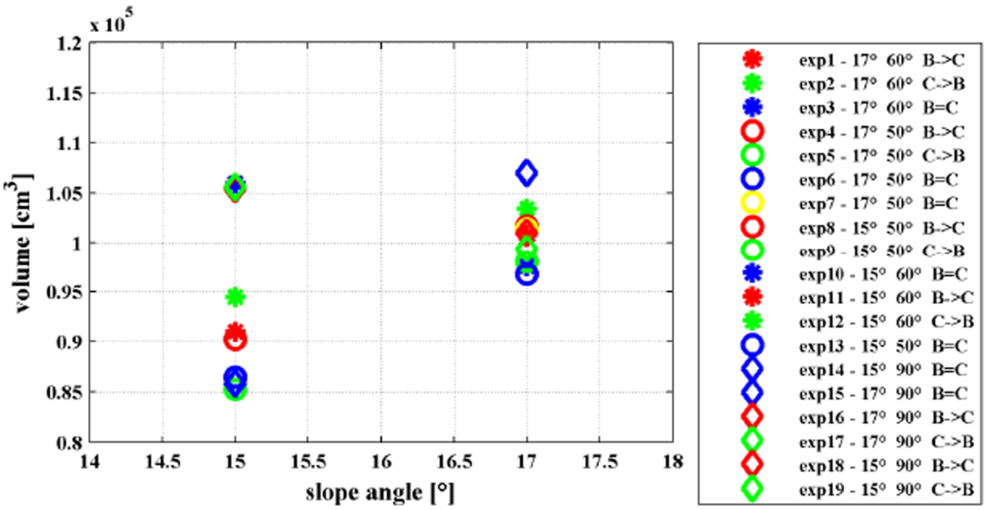

Figure 4 Volumes of the sediment deposit surveyed along the main channel at the end of each test versus the slope angle of the tributary channel.

the interaction between the two debris deposits (or fans). This is confirmed by the analysis on the overall deposit geometry described in the next section.

3.2 Analysis on the overall deposit geometry along the main channel

In order to assess the influence of the various parameters on the mutual interaction between the two deposits and on the possibility of generating a debris dam we have performed a systematic comparison between the plan view geometries of the sediment deposits surveyed at the end of each test. Figure 6 shows the contour lines of sediment levels z greater than 3.5 cm, observed for the three different triggering scenarios (I, Figure 6a, II, Figure 6b and III, Figure 6c), a tributary slope angle of 17° and confluence of 90°. It clearly appears how the triggering sequence plays an important role in terms of mutual interaction between the two debris fans. In particular, it is observed an increased tendency towards damming of the main channel section, moving from I to the III scenario.

Figure 7 shows the comparisons between tests characterized by the same confluence angle (90°) and triggering conditions (scenario I), for different tributary slopes (17°, Figure 7a and 15°, Figure 7b). The tests characterized by the higher slope displays a larger degree of obstruction in terms of both the overall extension of depositional area and shrinking of the main channel section.

Finally, Figure 8 shows the comparisons of tests characterized by the same slope angle (17°) and triggering scenario (III), for three values of the confluence angle (50°, Figure 8a; 60°, Figure 8b; 90°, Figure 8c). Increasing the confluence angle leads to large changes of the deposit shape. The debris fan generated by channel B moves downstream, while that produced by channel C is more elongated in the upstream direction, due to the interaction between the two deposits, leading to the deposition of a strip of material between the two main fans. The overall analysis of Figure 8 also emphasizes the role of the main channel flow in reworking the sediment delivered by the tributaries. Lower confluence angles (e.g., 50°) enhance the washing out of the material deposited by the debris flow, limiting the thickness of the sediment deposits. Although the volume of material mobilized by debris flows in the tributaries is always the same, the bulk concentration of the transported sediment-water mixture and the duration of the debris flow events are such that the ability of the main channel to wash out the debris increases as the tributary slope decreases (i.e., for lower debris flow concentration and for a more gradual delivery of sediment to the main channel).

The mutual interference between the two deposits, resulting in the formation of a deposit situated between of the two debris fans, increases for higher confluence angles and tributary slopes. On the other hand, the interference between the two deposits is strongly enhanced when the debris flows are triggered simultaneously in the two tributary channels.

3.3 Analysis on damming formation and comparison with the interference index in literature

The possibility of dam formation due to the debris flow injection in a receiving river with a smaller slope has been studied by different authors. The proposed critical indexes for dam formation are based on different factors which characterize the dynamic of both the tributary debris flow and collecting river reach (Dal Sasso et al. 2014).

In the following we will consider some critical indexes which have been set up from field data (Swanson et al 1985, 1986; Ermini et al. 2006; Dal Sasso et al. 2014) and laboratory tests (Dang et al. 2009). The Annual Constriction Ratio (ACR) proposed by Swanson et al. (1985, 1986) is based on the debris flow velocity U_s and the main channel width B_w:

$$ACR = \frac{U_s}{B_w}$$

and entails conditions favoring the blockage for $ACR > 100$.

The Dimensionless Flow Index (DFI) proposed by Ermini et al. (2006)considers the discharge of the debris flow, $U_s\, B_T\, D$, and the discharge of the receiving river with a return period of 5 years ($Q_{T=5\,yr}$):

$$DFI = \frac{U_s B_T D}{Q_{T=5\,yr}}$$

where B_T is the width of the tributary channel in which the debris flow takes place and D is the debris flow depth. The condition for blockage requires $DFI > 1$. This index has been subsequently modified by including also the effects of sediment rain size, d_{30}. According to Ermini et al. (2006) the blockage of the downstream channel collecting the tributary debris flow is likely to occur when the Dimensionless Constriction Index (DCI) is larger than 0.002. Where,

$$DCI = \frac{U_s B_T\, D\, d_{30}}{Q_{T=5\,yr}\, B_w}$$

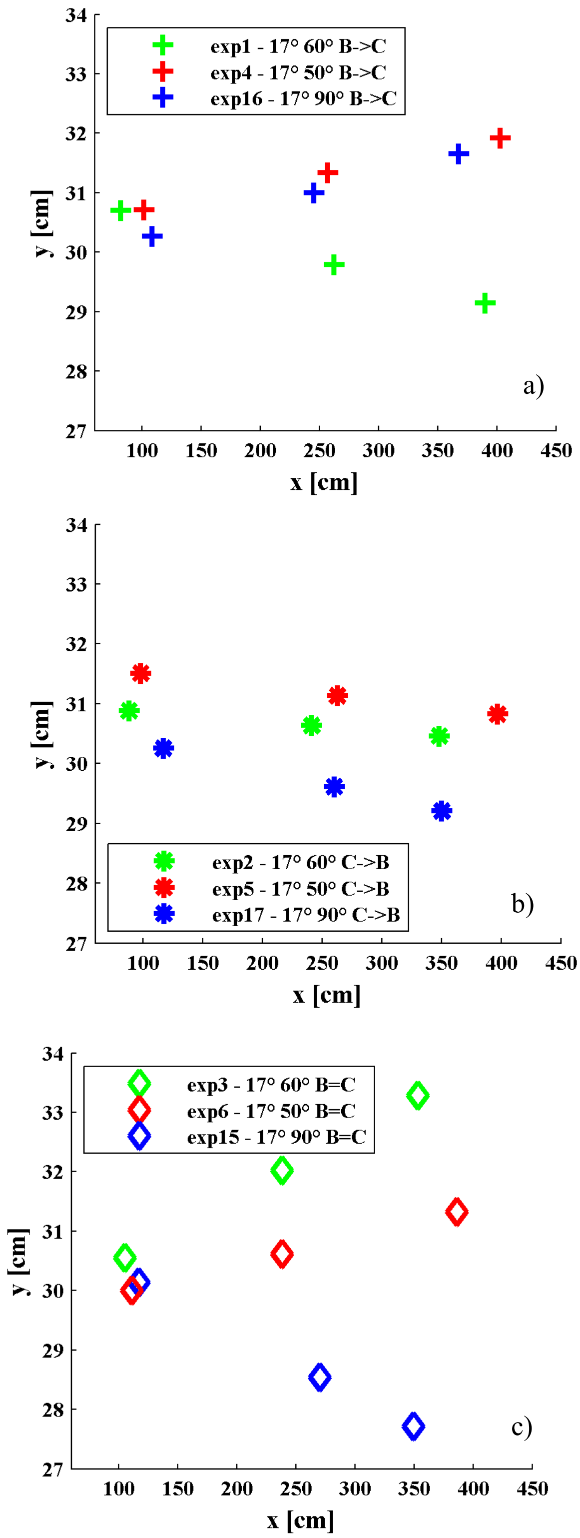

Figure 5 Center of mass of each debris fan (corresponding to the upstream and downstream confluences) and of the entire deposit for a slope angle of 17° and different confluence angle (50° -60° - 90°) varying the triggering scenario: a) triggering scenario I; b) triggering scenario II; c) triggering scenario III.

Recently, Dal Sasso et al. (2014) introduced the Dimensionless Morpho-Invasion Index (DMI), defined as the ratio of the debris flow momentum to the main river momentum:

$$DMI = \frac{2\rho_s U_s^2 V_s}{\rho_w g h^2 B_w B_r}$$

where ρ_s and ρ_w are the sediment and the water density, respectively, V_s is the debris flow volume, and h is the hydraulic level in the river. A complete damming is assumed to occur for DMI > 1.

Dang et al. (2009), on the basis of flume experiments, proposed a critical index based on the discharge ratio (R_Q = $Q_{debris\ flow}/Q_{river}$), the velocity ratio ($R_U$ = $U_{debrisflow}/U_{river}$), the bulk density ratio ($R_\gamma = \rho_s / \rho_w$) the sorting coefficient ($Sc = \sqrt{d_{75}/d_{25}}$) of the debris sediment, and the confluence angle, a. This index is defined as

$$CIDF = R_Q R_U R_\gamma Sc \sin a$$

For *CIDF* < 53.4 a semi-blockage of the main river section was observed, with the water flowing at one side of the main channel section; for 57 < *CIDF* < 71.5 a semi-blockage of the main river section was observed with the flow overpassing the deposited sediment; finally, for *CIDF* > 83.4 a complete blockage of the river section was observed.

In the case of the present flume experiments a partial obstruction of the main river section has been observed for the all tests. The higher degree of obstruction has been observed in the case of higher confluence and slope angles and with a simultaneous triggering scenario (III) (see Figure 8c). In the following we report the values attained by the above mentioned indexes, excluding however DFI and

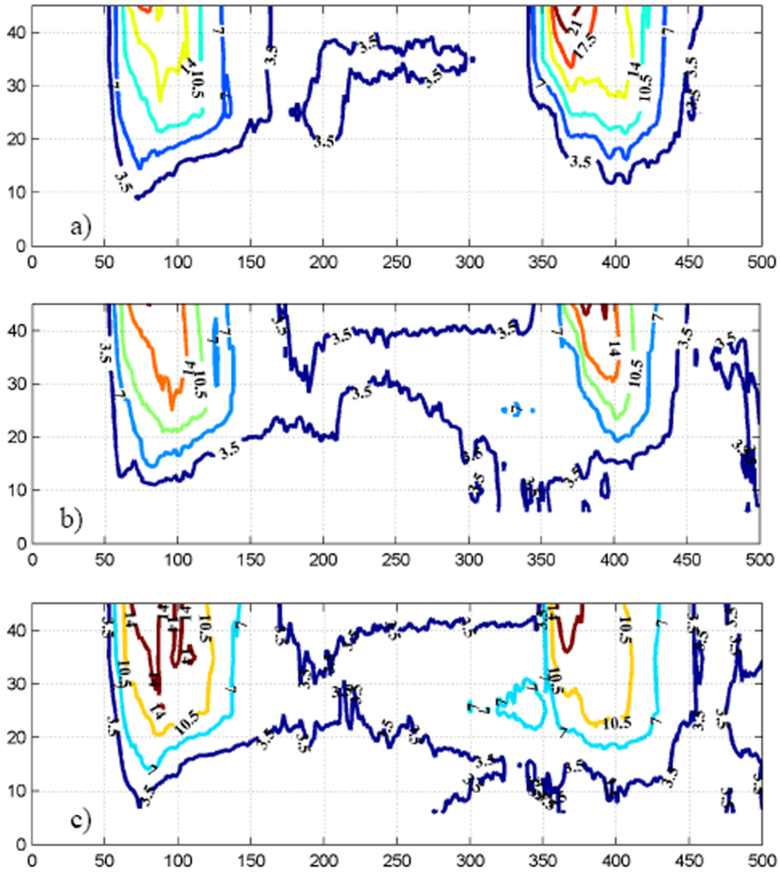

Figura 6 Top view of deposits along the main channel for a slope angle of 17° and confluence angles 90° varying the triggering scenario: a) triggering scenario I; b) triggering scenario II; c) triggering scenario III. Contour layers are expressed in cm above a threshold of 3.5 cm deposit level.

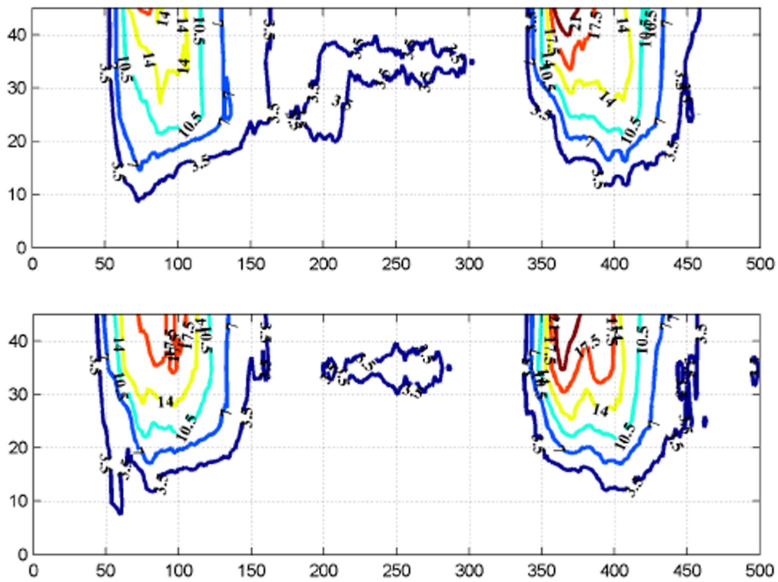

Figure 7 Top view of deposits along the main channel for a confluence angle of 90° and a triggering scenario I for different slope angles: 17° (upper), 15° (lower). Contour layers are expressed in cm above a threshold of 3.5 cm deposit level.

DCI, which involve the hydrologic estimate of $Q_{T=5\,yr}$, not applicable to the present experiments. The values computed for ACR (= 1.6) and CIDF (= 4 - 6) are consistent with our experimental findings indicating, for the range of parameter investigated, a semi-blockage of the river section. In particular the CIDF index indicate a type I blockage, with the water flowing at one side of the main channel section, as observed during the experiments (Figures 6 to 8). On the other hand, the value computed for DMI (about 110) would point at a complete blockage of the main channel, in contrast to the present experimental outcomes. This result poses a question on whether an index developed for assessing the mutual interference of a landslide (in which the role of the solid component is dominant) and a river can be applied to assess the interaction of a debris flow (in which the role of the fluid and the solid fractions are both fundamental) with the receiving stream.

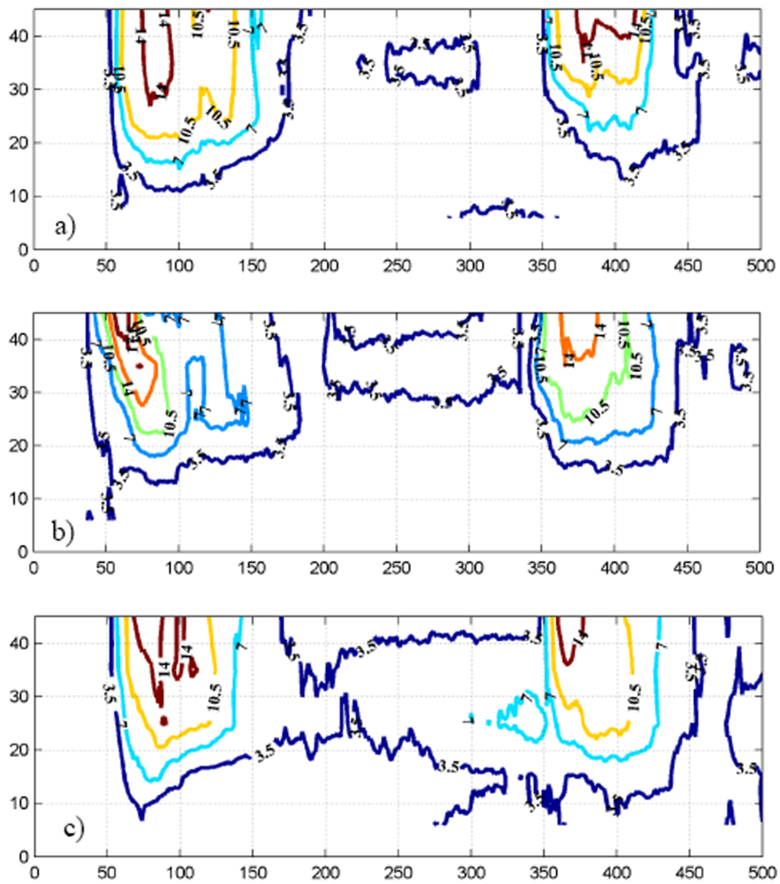

Figure 8 Top view of deposits along the main channel for a slope angle of 17° and a triggering scenario III for different confluence angles: (a) 50°; (b) 60°; (c) 90°. Contour layers are expressed in cm above a threshold of 3.5 cm deposit level.

In any case, all the indexes so far considered refer to the case of a single confluence and, hence, do not account for the role that the debris flow triggering sequence has in determining the shape of the overall sediment deposit, as discussed in the previous section. Keeping in mind that the obstruction configurations attained in the present experiments cover only one of the blockage types defined by Dang et al. (2009), we suggest that a possible extension of the CIDF index to the case of multiple and relatively close confluences can be easily obtained through the introduction of a multiplicative coefficient, φ, accounting for to the influence of the triggering scenario. This coefficient can be cast in the form:

$$\varphi = \varphi_s \left(1 + \frac{B_w}{L_c}\right)$$

where L_c is the inter-axis between the two confluences, and φ_s depends on the triggering conditions. For the conditions spanned by the present tests, entailing $0.1 < B_w/L_c < 1$, φ_s can be assumed equal to 0.6, 0.8 and 1 for the I, II and III triggering scenarios, respectively. Clearly, further tests are needed to better characterize this coefficient for the other two types of blockage listed by Dang et al. (2009), and to quantify how the mutual interaction between two confluences progressively decreases as their distance increases.

4 Conclusions

We have carried out an extensive series of laboratory experiments (19) aimed at understanding how the cross section of a mountain stream is affected by the sediment conveyed by lateral tributaries. Owing to the large slopes of these tributaries and the coarse grain size of the sediment, the transport mechanisms are those typical of stony debris flows, as those often observed on Italian Alps. The relevant parameters turn out to be the confluence angle, the tributary channel slope and the triggering sequence of debris flows. The deposit geometry surveyed at the end of each test and the characteristic parameters of the sediment deposit along the main channel, indicate that a significant washing out of sediment deposited in the receiving channel occurs for low confluence angle (50°) and low slope (15°). Conversely, wider and thicker sediment deposits are observed for perpendicular confluences (90°) and higher slopes (17°). The deposit geometry surveyed gives an overall estimate the degree of obstruction within the main channel. Indeed, it provides some information not only about the deposit generated by each confluence but also on the interference effects due to their interactions. Moreover, it has been observed that the more dangerous scenario, yielding a higher degree of obstruction, is attained in the experiments where debris flows are triggered simultaneously in the tributaries, no matter which confluence angle and slope configurations have been considered.

In conclusion, the risk of damming in a river reach as a consequence of lateral injections of the same volume of debris flow sediment tends to increase with the tributary slope and the confluence angle, and is the maximum if debris flows are triggered simultaneously. Further investigations are needed to quantify the degree of obstruction in the main channel in response to changes of the distance between the confluences, the volume of sediment available for the debris flow, as well as the size and the hydraulic regime of the main channel. In addition, although the present experiments, carried out using gravel, are deemed to be representative of stony debris flow conditions, the effects of a different granulometric composition of the sediment-water mixture, need to be studied including a certain amount of fine fractions.

Acknowledgement

The study is supported by the project GAPDEMM – GIS-based integrated platform for Debris Flow Monitoring, Modeling and Hazard Mitigation – founded by Fondazione Cassa di Risparmio di Padova e Rovigo in framework of Progetti di Eccellenza 2011-2012.

References

Benda L (1990) The influence of debris flows on channels and valley floors in the Oregon Coast Range, U.S.A. Earth Surf. Process. Landforms 15: 457-466. DOI: 10.1002/esp. 3290150508

Chen RD, Liu XN, Cao SY, Guo ZX (2011) Numerical simulation of deposit in confluence zone of debris flow and mainstream. Science China Technological Sciences 54: 2618-2628. DOI: 10.1007/s11431-011-4510-1

Chen SC, Peng SH, Capart H (2004) Morphology of alluvial fans formed by hyperconcentrated tributaries. In: Greco, M. et al. (eds.), Proceedings of the 2nd International Conference on Fluvial Hydraulics, Napoli, Italy. pp. 1095-1102. ISBN: 9058096882, 9058096580.

Cheng Z, Dang C, Liu J, Gong Y, (2007) Experiments of Debris Flow Damming in Southeast Tibet. Earth Science Frontiers 14: 181-185. DOI: 10.1016/S1872-5791(08)60010-X

Dal Sasso SF, Sole A, Pascale S, et al. (2014) Assessment methodology for the prediction of landslide dam hazard. Natural Hazards Earth System Science 14: 557-567. DOI: 10.5194/nhess-14-557-2014.

Dang C, Cui P, Cheng ZI (2009) The formation and failure of debris flow-dams, background, key factors and model tests: case studies from China. Environmental Geology 57:1901-1910. DOI: 10.1007/s00254-008-1479-6.

Ermini L, Casagli N, Farina P (2006) Landslide dams: analysis of case histories and new perspectives from the application of remote sensing monitoring techniques to hazard and risk assessment. Italian Journal Geology and Environment 1: 45-52. DOI: 10.4408/IJEGE.2006-0.1.S-05

Gregoretti C, Dalla Fontana G (2008) The triggering of debris flows due to channel - bed failure in some alpine headwater basins of Dolomites: analyses of critical runoff. Hydrological Processes 22: 2248-2263. DOI: 10.1002/hyp.6821

Lanzoni S, Tubino M (1993) Rheometric experiments on mature debris flows. In: Proceedings XXV IAHR Congress, Tokyo, Japan. 3: pp 47-54.

Li Y, Su P, Cui P, Hu K (2008) A probabilistic view of debris flow. Journal of Mountain Science 5: 91-97. DOI: 10.1007/ s11629-008-0111-2.

Rickenmann D, Recking A (2011) Evaluation of flow resistance in gravel- bed rivers through a large field data set. Water Resources Research, 47, W07 538. DOI: 10.1029/2010WR 009793.

Swanson FJ, Graham RL, Grant GE (1985) Some effects of slope movements on rver channel. In: International Symposium on Erosion, Debris Flow and Disaster Prevention, Proceedings: Tsukuba, Japan. Erosion Control Engineering Society of Japan. pp 273-27.

Swanson FJ, Oyagi N, Tominaga M (1986) Landslide dam in Japan. In: Landslide Dam: Processes Risk and Mitigation. In: Schuster RL (Ed.), American Society of Civil Engineers, Geotechnical Special Publication 3: 131-145.

Takahashi T (2007) Debris Flow. Rotterdam: Balkema. Taylor & Francis, London, UK. ISBN: 978-0-415-43552-9

Zhou JW, Cui P, Yang XG, et al. (2013) Debris flows introduced in landslide deposits under rainfall conditions: The case of Wenjiagou Gully. Journal of Mountain Science 10(2): 249-260. DOI: 10.1007/s11629-013-2492-0